1   # Molecular characterization of organic aerosol in Himalayas: insight from

2   # ultra-high resolution mass spectrometry

3   Yanqing An[1], Jianzhong Xu[1], Lin Feng[1, 2], Xinghua Zhang[1, 2], Yanmei Liu[1, 2], Shichang Kang[1,2]

4   [1]State Key Laboratory of Cryospheric Science, Northwest Institute of Eco-Environment and

5   Resources, Chinese Academy of Sciences, Lanzhou 730000, China

6   [2]University of Chinese Academy of Sciences (UCAS), Beijing 100049, China

7   Corresponding Author: Jianzhong Xu, jzxu@lzb.ac.cn

Atmospheric
Chemistry
and Physics
Discussions

8 **Abstract**

9 An increasing trend in aerosol concentration has been observed in Himalayas in recent years, but

10 the understanding of the chemical composition and sources of aerosol remains poor. In this

11 study, molecular chemical composition of water soluble organic matter (WSOM) from two filter

12 samples (denoted as F30 and F43) collected during high aerosol loading periods at a high altitude

13 station (Qomolangma Station, QOMS, 4276 m a.s.l.) in the northern Himalayas were identified

14 by positive electrospray ionization Fourier transform ion cyclotron resonance mass spectrometry

15 (ESI-FTICR-MS). More than 4500 molecular formulas were identified in each filter sample

16 which were classified into two compound groups (CHO and CHON) based on their elemental

17 composition with both accounting for nearly equal contributions in number (45% – 55%). The

18 relative abundance weighted mole ratio of O/C_w for F30 and F43 are 0.43 and 0.38, respectively,

19 and the weighted double bond equivalent (DBE_w), an index for the saturation of organic

20 molecules, were 6.26 and 6.92, respectively, suggesting their medium oxidation and saturation

21 degrees. Although the O/C_w mole ratio was comparable for CHO and CHON compounds, the

22 DBE_w was significant higher in CHON compounds than CHO compounds. More than 50%

23 molecular formulas in Van Krevelen (VK) diagram (H/C vs. O/C) located in 1 – 1.5 (H/C) and

24 0.2 – 0.6 (O/C) regions, suggesting potential lignin-like compounds. The distributions of CHO

25 and CHON compounds in VK diagram, DBE vs. number of C atoms, and other diagnose

26 diagrams showed highly similarities between each other suggesting their similar source and/or

27 atmospheric processes. Detailed molecular information in the common formula of these two

28 filters was explored. Many formulas with their homologous series of compounds formed from

29 biogenic volatile organic compounds and biomass mass burning emitted compounds were found

30 in the WSOM with high relative abundance suggesting the important contribution of these two

31 sources in Himalayas. The high DBE and high nitrogen containing of aerosol would have

32 important implication for aerosol light absorption and biogeochemical cycle in this remote

33 region.

34

Atmospheric
Chemistry
and Physics
Discussions

1. Introduction

Elevated pollutant concentrations has been frequently observed over Himalayas during pre-monsoon period (March to June) (Bonasoni et al., 2010). The high aerosol loading plume are originated from the southern regions of Himalayas such as northwestern India and/or Indian Gangetic region based on air mass back trajectory analysis and satellite observation (Liu et al., 2008; Lu et al., 2012; Lüthi et al., 2015). In recent decades, due to increased consumption on fuels (including biofuels and fossil fuels) by industry and residents, air pollution has been a serious issue in South Asia (Gustafsson et al., 2009). Accompany with favorable atmospheric circulation, air pollutants emitted or formed in these regions can be fast transported to Himalayas and Tibetan Plateau (HTP) (Xia et al., 2011).

Elevated aerosol concentration for the pristine region of the HTP is thought to have essential climate and environment effects. For example, the transported aerosol could heat the air at the higher layer of troposphere over the HTP and impact on the monsoon system of south Asia and accelerate the melting of glacier in Himalayas (Lau et al., 2006; Ramanathan et al., 2007). This heating effect is predominantly from the light absorbing particular aerosol (LAPA) such as black carbon (BC) and brown carbon which is part of organic aerosol (OA) (Ram et al., 2010; Zhang et al., 2015; Zhang et al., 2017). BC come from incomplete combustion and dominates the absorption of LAPA; Brown carbon could from many processes such as primary emission and secondary process and have an increasing contribution (up to ~20%) to the light absorption in recent years (Laskin et al., 2015). Many studies show that open biomass burning is an important source of BC and brown carbon (e. g., Saleh et al., 2014), which is very popular in developing regions in the southern of Himalayas. However, high elevation and mixed biomass fuels in these regions could make the evolution of biomass burning emission more complicated and the chemical information of OA remains poorly characterized so far (Fleming et al., 2018).

The details on the molecular composition of OA are important for understanding the sources and chemical evolution of OA (Laskin et al., 2018). Previous studies conducted in the HTP have focused on a limited number of molecular markers such as organic acids which are closely related with biomass burning emission (Cong et al., 2015), and some toxicology species such as

Atmospheric
Chemistry
and Physics
Discussions

Open Access

EGU

65 polycyclic aromatic hydrocarbons (PAHs) and persistent organic pollutants (POPs) which are

66 related with anthropogenic activities (Wang et al., 2015; Wang et al., 2016). In addition, online

67 measurement using Aerodyne high resolution time-of-flight aerosol mass spectrometer (HR-

68 ToF-AMS) had provided more details on the OA chemistry and sources with high time

69 resolution (Xu et al., 2018). However, different instrument has its limitations on OA detection

70 and ultra-high mass resolution of mass spectrometry which can identify a large number of

71 molecular formulas is lacking.

72

73 Electrospray ionization (ESI) with ultrahigh-resolution Fourier transform-ion cyclotron

74 resonance mass spectrometry (FTICR-MS) can be used to identify the individual molecular

75 formula of complex mixture because of its extremely high resolution and mass accuracy

76 (Mazzoleni et al., 2010). In this study, we focus on the comprehensive characterization of the

77 molecule composition of water soluble organic compound in fine particle aerosol collected in the

78 northern slope of central Himalayas using positive mode ESI-FTICR-MS.

79

80 **2. Methodology**

81 **2.1. Aerosol sampling**

82 Field study was conducted at the Qomolangma Station (QOMS, 28.36° N, 86.95° E, 4276 m

83 a.s.l.) located at the toe of Mt. Qomolangma from Apr. 12 to May 12, 2016 using a suit of

84 instruments (Zhang et al., 2018b), and the instruments used in this study includes a HR-ToF-

85 AMS (Aerodyne Research Inc., Billerica, MA, USA) for 5-min size-resolved chemical

86 compositions (organics, sulfate, nitrate, ammonium, and chloride) of non-refractory submicron

87 particulate matter (NR-PM$_1$) and a photoacoustic extinctionmeter (PAX, DMT Inc., Boulder,

88 CO, USA) for BC mass concentration. The QOMS observatory locates at a remote site with

89 sparse local residents and anthropogenic activities around it, except for a high way for the

90 tourism to the west about 500 m. The tourists are normally increased from June each year due to

91 the warmer weather during summer. The weather at the QOMS during the field study was

92 dominated by westerlies with the prevailed wind from west and southwest with an average air

93 temperature of 5.7 ± 5.0 °C. A low-volume (16.7 L min^{-1}) particular matter (PM) sampler (BGI,

94 USA, model PQ 200) with an aerodyne diameter cutoff of 2.5 μm at the inlet was used to collect

95 PM$_{2.5}$ filter samples on pre-baked quartz fiber filters (47 mm, Pall Life Science, NY, USA). Due

96 to the low aerosol loading at this remote region, two days sampling strategy was adapted for each

97 filter collection starting from 8:00 am to 7:45 am at the day after tomorrow (local time). A total

98 of 18 filter samples were collected during the field study with three procedure blanks which were

99 used to assess potential contamination during sampling and transportation. The sampling air

100 volume ranged from 35.1 to 48.1 m^3 at ambient conditions. Two filter samples collected during

101 Apr. 25 – 27 (F30) and Apr. 29 – May 1 (F43) were chosen in this study due to the relative

102 higher aerosol loading based on HR-ToF-AMS results (section 3.1) and distinct particulate

103 matter on the filter. In addition, the temporal variations of aerosol concentration recorded by HR-

104 ToF-AMS during these two filter periods shown a smoothly increase indicating a regional

105 transportation which could be typical long-range transport events at this region.

106

107 **2.2. Chemical analysis**

108 For FTICR-MS analysis, these two filters were firstly extracted in 20 mL Milli-Q water in an

109 ultrasonic bath for 30 min and filtered using 0.45 µm pore-size Acrodisc syringe filters to

110 remove water insoluble matter (Pall Science, USA). Prior to FTICR-MS analysis, the extraction

111 was concentrated and purification using PPL (Agilent Bond Elut-PPL cartridges, 500 mg, 6 mL)

112 solid phase extraction (SPE) cartridges for water soluble organic matter (WSOM). Note that

113 through SPE cartridge, the most hydrophilic compounds such as inorganic ions, and low-

114 molecular-weight organic molecules such as organic acids and sugars were removed, whereas

115 the relatively hydrophobic fraction was retained. The details on the SPE method using PPL

116 cartridges and analysis by FTICR-MS can be found in our previous paper (Feng et al., 2016).

117 Briefly, the mass spectrometry analyses of these samples were performed using a SolariX XR

118 FT-ICR-MS (Bruker Daltonik GmbH, Bremen, Germany) equipped with a 9.4 T refrigerated

119 actively shielded superconducting magnet (Bruker Biospin, Wissembourg, France) and a Paracell

120 analyzer cell. The samples were ionized in positive ion modes using the ESI ion source (Bruker

121 Daltonik GmbH, Bremen, Germany). A typical mass-resolving power of >400 000 was achieved

122 at m/z 400 with an absolute mass error of <0.5 ppm. Molecular formulas were assigned to all

123 ions with signal-to-noise ratios of greater than 10 with a mass tolerance of ±1.5 ppm using

124 custom software. Molecular formulas with their maximum numbers of atoms were defined as: 30

125   ^{12}C, 60 ^{1}H, 20 ^{16}O, 3 ^{14}N, 1 ^{32}S, 1 ^{13}C, 1 ^{18}O and 1 ^{34}S. Identified formulas containing

126   isotopomers (i.e., ^{13}C, ^{18}O or ^{34}S) were not considered. Compounds were detected as either

127   sodium adducts, [M + Na]$^{+}$, or protonated species, [M + H]$^{-}$. We report all detected compounds

128   as neutral species, unless stated otherwise.

129

130   **2.3. Data processing**

131   The assigned molecular formulas were examined using the van Krevelen diagram (Wu et al.,

132   2004), double-bond equivalents (DBEs), Kendrick mass defects (KMD) series, and aromatic

133   indices (AI$_{mod}$). The O/C and H/C ratios were calculated by dividing the number of O and H

134   atoms, respectively, by the number of C atoms in a formula. DBE analysis was used to determine

135   the number of rings and double bonds in a molecule. The DBE was calculated using equation 1,

136   $DBE = 1 + c - h/2 + n/2,$ (1)

137   where c, h, and n are the numbers of C, H, and N atoms, respectively, in the formula.

138

139   The KMD can be used to search for potential oligomeric units (Hughey et al., 2001). The

140   Kendrick mass (KM) and KMD for CH$_2$ series were calculated using equations 2 and 3,

141   $KM = observed\ mass \times 14/14.01565,$ (2)

142   $KMD = NM - KM,$ (3)

143   where 14 is the nominal mass (NM) of CH$_2$, 14.01565 is the exact mass of CH$_2$, and NM is KM

144   rounded to the nearest integer. A homologous series of compounds differing only by the number

145   of base units form a horizontal line in a plot of KMD against KM.

146

147   AI$_{mod}$ is a measure of the probable aromaticity of a molecule assuming that half the O atoms are

148   double bonded and half have only σ bonds (Koch and Dittmar, 2006). AI$_{mod}$ was calculated using

149   equation 4,

150   $AI_{mod} = (1 + c - 0.5o - 0.5h) / (c - 0.5o - n),$ (4)

151   where c, o, and h are the number of C, O, H, and N atoms in the formula. AI$_{mod}$ ranges from 0 for

152   a purely aliphatic compound to higher values being found for compounds with more double

153   bonds and that are more aromatic.

154

3. Results and discussions

3.1. Chemical characterization of PM_1 during F30 and F43 measured by HR-ToF-AMS

The average mass concentration and chemical composition measured by HR-ToF-AMS during F30 and F43 periods were shown in Fig. 1. The mass concentration of PM_1 were 9.2 and 10.6 μg m^{-3}, respectively, which were at the high range of all filters (1.3 – 10.6 μg m^{-3}) because of a continuous long-range transport event at the QOMS (Zhang et al., 2018b). Due to our sample processing error, the mass concentration of filter measured gravimetrically could not be used and thus the fractions of PM_1 to $PM_{2.5}$ are not available. However, most of WSOM in $PM_{2.5}$ is in accumulation size mode (less than 1μm) which could be detected by HR-ToF-AMS. The chemical composition of PM_1 during F30 and F43 were all dominated by OA (55% and 57%), followed by BC (26% and 22%), sulfate (7% and 8%), nitrate (5% and 6%), and ammonium (5% and 6%). The OA was comprised by biomass burning emitted OA (BBOA), nitrogen-contained OA (NOA), and more-oxidized oxygenated OA (MO-OOA) decomposed by positive matrix factorization (PMF) analysis (Fig. 1). The mass contribution of BBOA was higher during F43 than F30 (32% vs. 22%), whereas the contribution of MO-OOA was higher during F30 than F43 (24% vs. 16%). The mass spectra of OA for these two filter periods were closely similar with a person correlation efficiency (*r*) being 0.9. The elemental ratios of oxygen (O) to carbon (C) of OA were 1.04 and 0.97 for F30 and F43 periods (IA method, Canagaratna et al., 2015), respectively, and accordingly the ratios of hydrogen (H) to C were 1.26 and 1.32. These suggest that the OA during F43 was relatively less oxidized than that during F30 (*t*-test, p<0.05). The six category ions ($C_xH_y^+$, $C_xH_yO_2^+$, $C_xH_yO_1^+$, $C_xH_yN^+$, $C_xH_yO_zN^+$, and HO^+) detected by HR-ToF-AMS for these two filter periods were all dominated by $C_xH_yO_2^+$, following by $C_xH_y^+$, $C_xH_yO_1^+$, $C_xH_yN^+$, $C_xH_yO_zN^+$, and HO^+. The air mass trajectory analyses using the hybrid single particle Lagrangian integrated trajectory (HYSPLIT) model for F35 and F43 periods show air mass mainly originated from west and southwest of the QOMS across north and northwest India where there were many fire spots during these two periods (Fig. 2). The air mass during F43 was partly (13%) transport with low wind speed and short distance (less than 100 km) indicating some potential fresh OA.

184   **3.2. The chemical characteristics of WSOM from ESI-FTICR-MS**

185   A total of 4554 and 5192 molecular formulas was identified by ESI(+)-FTICT-MS over the mass

186   range of 100-700 Da for F30 and F43, respectively. The identified molecular formulas were

187   grouped into two subgroups based on their elemental composition, i.e., CHO and CHON, all of

188   which had equal important contribution (45% – 55%) in number (Fig. 3). Note that individual

189   species in the ESI-FTICR-MS mass spectra could have many different isomeric structures, then

190   the percentages reflect only the number of unique molecular formulas and do not reflect the

191   number of unique molecular formulas in each category. Although there exists the difference on

192   ionization sensitivity of ESI(+) between different studies, the contribution of CHON in our study

193   is higher than the results before (10% - 30%) (Laskin et al., 2009; Dzepina et al., 2015). The

194   distinct contribution of CHON compounds in ESI-FTICR-MS mass spectra is consistent with the

195   results of HR-ToF-AMS which identified a separate NOA factor in PMF analysis. The mass

196   spectra of these two samples were highly similar in the distributions of molecular relative

197   intensity (RI) (Fig. 3). The most abundant peaks were a series of CHO compounds cationized by

198   Na^+ (RI>20%, $C_{19}H_{28}O_3(C_2H_4O)_{n=0-6}Na^+$). These compounds were most likely to contain

199   carboxylic acid groups that readily form $[M + Na]^+$ ions in the positive mode electrospray

200   ionization (Smith et al., 2009). The average weighted element ratios of F30 and F45 were 0.43

201   vs. 0.38 for O/C_w, 1.38 vs. 1.33 for H/C_w, and 1.72 vs. 1.67 for OM/OC_w (Table 1), suggesting a

202   relative higher oxidation and saturation degree for F30 than F43. These trends are similar with

203   those of HR-ToF-AMS results, although the elemental ratios are different between them which is

204   due to the difference on the detection range of m/z and the ionization efficiency of different mass

205   spectrometry (ESI vs. EI) (Yu et al., 2016). The elemental ratios of WSOM from ESI-FTICR-

206   MS in our study are similar with those results observed in aerosol samples in remote site using

207   ESI-FTICR-MS (e.g., 0.35 – 0.53 for O/C) (Table 2). The CHO compounds had relatively higher

208   O/C_w ratio than that of CHON compounds in these two samples and CHO compounds were more

209   saturated with a higher H/C_w ratio than CHON (Table 1). The O/C and H/C in Van Krevelen

210   diagrams (Wu et al., 2004) for these two filters and the subgroup molecular show similar

211   distributions and all concentrate in 1.2-1.8 for H/C and 0.3-0.7 for O/C (Fig. 3) suggesting their

212   similar aerosol sources and atmospheric processes. The similar distributions for these two filters

213   are also observed in KMD vs. KM plots and located in a narrow and uniform distribution, which

214   are similar with highly processed aerosol found at the Pico Mountain Observatory (Dzepina et

215   al., 2015).

216

217   Structural information for the assigned molecular formulas is inferred from the DBE_w value

218   which was higher for F43 than that of F30 (6.92 vs. 6.26) (Table 1). Comparing with other

219   studies, the DBE values in our filter is relative lower than those in fresh emitted aerosol from

220   fuel combustion (5 − 9.5) (Song et al., 2018), but close to the results from biomass burning

221   aerosol and aerosol samples from remote sites (Table 2) (Dzepina et al., 2015). The DBE_w values

222   for each molecule subgroup were higher for CHON than that of CHO (Table 1), especially for

223   F43 (7.46 vs. 6.69) suggesting more rings and double bonds in CHON molecular. The AI_{mod},

224   reflecting the minimum number of carbon-carbon double bonds and rings (Koch and Dittmar,

225   2006), was correspondingly higher in F43 which contained 49.1% aliphatic (60.4% in F30),

226   45.9% olefinic (36.8% in F30), and 5.1% aromatic compounds (2.9% in F30). For aromatic

227   compounds (AI_{mod} >=0.5) in F43, ~60% of them were CHON formulas (39% for F30) (Table 1).

228   A distinct group of CHON aromatic compounds is shown in lower left corner in Van Krevelen

229   diagram for F43 but not for F30 (Fig. 3). Higher DBE and AI_{mod} values in CHON compounds

230   suggest more unsaturated compounds with them which could contain a certain number of

231   chromophores. The distribution of DBE vs. carbon number of two filters showed a systematic

232   increase in a concentrated region and a highly similarity with each other. This similarity further

233   suggests the consistent source and chemical processes for the aerosol of these two filters.

234

235   There were 3700 common molecular formulas between these two filters with the number

236   contribution of CHO by 47% and CHON by 53%. These common molecular formulas accounted

237   for 81% (F30) and 71% (F43) of two filters, respectively. There were 619 unique molecular

238   formulas in F30 with 91% being CHO compounds; whereas there were 1142 unique molecular

239   formulas in F43 with 62% being CHON compounds. For more confidence on molecule

240   assignment, we focus on the common molecular formulas detected in these two samples in the

241   section below.

242

Atmospheric
Chemistry
and Physics
Discussions

3.3. The potential sources and formation processes

3.3.1. CHO compounds

243 **3.3. The potential sources and formation processes**

244 **3.3.1. CHO compounds**

245 CHO compounds have been frequently detected in ambient aerosol samples (Altieri et al., 2009a;

246 Mazzoleni et al., 2010; Lin et al., 2012; Fleming et al., 2018), which could comprise of high

247 molecule weight humic-like substances (HULIS) or oligomers, and from primary emission or

248 secondary formation of different aerosol sources (Mazzoleni et al., 2012; Wozniak et al., 2014;

249 Lin et al., 2016; Cook et al., 2017). In our samples, the weighted molecule weight of CHO

250 compounds was 363.7 with an average C atom of 19.1 ± 5.3 per molecule; the most abundant O

251 atoms located in 5-10 with an average value of 7.6 ± 2.9 per molecule (Fig. 4a and b). Among

252 the 1744 common CHO formulas, 388 of them (22%) are observed as $[M + Na^+]$ ions with the

253 majority of detected as protonated species. The most abundant sodiated molecules in the ESI/MS

254 ranged in m/z 350-550, whereas the most abundant protonated species ranged in m/z 200-350.

255 The DBE of CHO increased with the carbon number with the DBE_w being 5.96 (Fig. 3); the

256 carbon-normalized DBE_w (DBE/C_w) was 0.33 (Table 1). These two values were close to the

257 results from biomass burning aerosol samples in other studies (Table 2) (Lin et al., 2012;

258 Mazzoleni et al., 2012). A threshold DBE/C value of 0.7 usually serves as a criterion to identify

259 species with condensed aromatic ring structures and therefore the CHO compounds in our

260 samples were relative low aromaticity likely due to the relative long oxygenation time during

261 long-range transport. The Carbon oxidation state (OSc) values (Kroll et al., 2011), a useful

262 metric for the degree of oxidation of organic species in the atmosphere, exhibited between -1 and

263 0 with 25 or less carbon atoms, suggesting that they are semi- and low-volatile organic

264 compounds corresponding to "fresh" (BBOA) and "aged" (LV-OOA) SOA by multistep

265 oxidation reactions (Fig. 4c).

266

267 There are several possible sources and chemical formation pathways for high oxygen-containing

268 CHO compounds. Ozonolysis of α-pinene has been found to form highly oxygenated molecules,

269 and one of the products is $C_{17}H_{26}O_8$ (m/z 358) (RI = 9.2%) and $C_{19}H_{28}O_7$ (m/z 368) (RI = 3.2%)

270 which is a possible esterification product of cis-pinic ($C_9H_{14}O_4$, m/z 186, RI = 7.2%) and

271 diaterpenylic acid ($C_8H_{14}O_5$, m/z 190) (Kristensen et al., 2013). The first three compounds were

272 all found in the common CHO molecules with high relative abundance and ionized by Na^+.

Atmospheric
Chemistry
and Physics
Discussions

273   Ozone concentration in Himalayas during pre-monsoon was highest based on the on-line

274   measurement at the Nepal Climate Observatory at Pyramid (NCO-P) during 2006-2008 (61 ± 9

275   ppbv) (Cristofanelli et al., 2010). High biogenic volatile organic compound emissions could

276   occur due to high density of forest in the southern Himalayas and biogenic secondary organic

277   aerosol has been found to be important source in Himalayas (Stone et al., 2012). A number of

278   previously reported other monoterpene oxidation products were also observed in our study, such

279   as $C_6H_{10}O_5Na^+$ (RI = 1.3%), $C_8H_{10}O_5Na^+$ (RI = 3.9%), $C_8H_{12}O_5H^+$ (RI = 6.7%), $C_9H_{14}O_5H^+$ (RI

280   = 5.4%), $C_{10}H_{14}O_6Na^+$ (RI = 7.7%), $C_{10}H_{14}O_7Na^+$ (RI = 8.4%), $C_9H_{12}O_6Na^+$ (RI = 3.4%),

281   $C_7H_{10}O_5Na^+$ (RI = 2.9%), $C_{10}H_{16}O_3H^+$ (RI = 3.8%), $C_7H_{10}O_5Na^+$ (RI = 1.8%), $C_7H_{12}O_5Na^+$ (RI =

282   2.0%), $C_8H_{12}O_6Na^+$ (RI = 6.7%) (Claeys et al., 2007; Kleindienst et al., 2007; Zhang et al.,

283   2018a). We also observed formulas that could be lignin pyrolysis products such as vanillic acid

284   ($C_8H_8O_4H^+$, RI = 1.1%), syringaldehyde ($C_9H_{10}O_4H^+$; RI = 2.1%), and syringic acid ($C_9H_{10}O_5H^+$;

285   RI = 2.7%). In addition, Sun et al. (2010) and Yu et al. (2014; 2016) observed that aqueous-

286   phase oxidation of lignin produces phenol (C_6H_6O), guaiacol ($C_7H_8O_2$) and syringol ($C_8H_{10}O_3$)

287   yields a substantial fraction of dimers and higher oligomers with key dimer markers identified as

288   $C_{16}H_{18}O_6$ and $C_{14}H_{14}O_4$. The dimer markers $C_{16}H_{18}O_6H^+$ and $C_{14}H_{14}O_4H^+$ were also present in

289   our sample with high RI (7.6% and 7.8%) and $C_{16}H_{18}O_6Na^+$ was also observed (RI = 1.5%). The

290   high relative intensity of these compounds indicate that fog and cloud processing of phenolic

291   species (biomass burning aerosol) could be an important mechanism for the production of low-

292   volatility SOA in Himalayas. Some other biomass burning emission compounds were also found,

293   such as dicarboxylic acid series $C_6H_{10}O_4(CH_2)_nH^+$ and dihydroxycarboxylic acids

294   $C_9H_{18}O_4(CH_2)_nH^+$; A series of saturated $C_{16}H_{12}O_8(CH_2)_nH^+$ ketones were also observed in the

295   sample (Fig. 4d). Compounds ($C_9H_{10}O_3H^+$, $C_{10}H_{10}O_3H^+$, $C_{11}H_{10}O_3H^+$, $C_{11}H_{12}O_3H^+$, $C_{12}H_{12}O_2H^+$,

296   $C_{13}H_{12}O_3H^+$, $C_{13}H_{14}O_3H^+$, $C_{13}H_{14}O_4H^+$, $C_{14}H_{16}O_4H^+$, $C_{14}H_{16}O_3H^+$) observed in biomass burning

297   emission (cow dung and brush wood) sampling during residential cooking in Nepal (Fleming et

298   al., 2018) were also found in our samples.

299

300   **3.3.2 CHON compounds**

301   The frequency distribution for n_o and n_c in CHON formulas were shown in Fig. 5a which show

302   peaks between 6-10 and 15-20, respectively. The DBE of CHON formulas ranged into 4 – 10

Atmospheric
Chemistry
and Physics
Discussions

303   with DBE_w being 6.79 (Fig. 5b). In the $CHON^+$ class, compounds contained one or two nitrogen

304   (1N or 2N) atoms with 1N compounds accounting for 70.5% and 2N for 29.5%, respectively.

305   Most (98%) of 1N compounds contained more than 3 oxygen atoms and could up to 13 oxygen

306   atoms, whereas about 62.5% of 2N compounds contained more than 6 oxygen atoms (Fig. 6a).

307   The average O atom containing in each molecular formula was therefore higher for 1N

308   compounds than 2N compounds (8.1 ± 2.9 vs. 6.3 ± 2.3). The high O atom containing in CHON

309   formula suggest that nitrogen was in the form of organic nitrate or nitro groups with excess

310   oxygen forming additional oxygenated groups. The ratios of O/C_w and OSc_w for 1N compounds

311   were accordingly higher than that of 2N compounds (0.42 vs. 0.37 for O/C_w; -0.48 vs. -0.54 for

312   OSc_w), suggesting higher oxidation state for 1N compounds (Fig. 5c). In contrast, the DBE_w and

313   AI_{mod} values for 2N compounds were higher than that of 1N compounds (Table 1). With higher

314   H/C_w for 2N compounds (Table 1), it suggests that 2N compounds could contain amount of

315   aromatic N-heterocyclic compounds. For 1N compounds, longer and higher relative intensity

316   CH_2 homologous series compounds were found based on the Kendrick mass defect plot (Fig.

317   6b); 1073 of the 1378 detected 1N compounds can be grouped into 145 homologous. The

318   abundant long CH_2 homologous series in 1N compounds contained 7-10 O atoms, while 5-8 O

319   atoms for 2N compounds (Fig. 6).

320

321   There are many potential sources for CHON compounds, such as amino acids, reduced N

322   compounds, nitro compounds, and organic nitrate (Altieri et al., 2009b; Laskin et al., 2009;

323   O'Brien et al., 2013). Biomass burning has been found to be an important source for nitrogen-

324   containing compounds in atmosphere (Hoffmann et al., 2007). Laskin et al. (2009) identified

325   amount of N-heterocyclic alkaloid compounds from kinds of fresh biomass burning aerosol.

326   Fleming et al. (2018) conducted study in Nepal by collecting fresh emitted aerosol from dung

327   and brushwood burning household cookstoves and identified amount of nitrogen-containing

328   aerosol. Oxygenated organic nitrogen compounds in ambient aerosol (Dzepina et al., 2015), rain

329   water (Altieri et al., 2009b), and fog water (Mazzoleni et al., 2010) from biomass burning

330   emission influenced regions were also observed. Although the dominated CHN compounds in

331   fresh aerosol in Laskin et al. (2009) and Fleming et al. (2018) were not found in our study which

332   was likely due to the highly oxygenated OA in our samples, biomass burning emissions could be

Atmospheric
Chemistry
and Physics
Discussions
Open Access

EGU

333   an important source for CHON compounds in our study. Recent studies have proven that burning

334   of dung-fuel in Nepal can emit amount of nitrogen species such as NH_3, NO_x, HCN, benzene,

335   and organics, and the emission factors for these species are higher than that of wood (Stockwell

336   et al., 2016; Jayarathne et al., 2018). In addition, it is likely that smoldering burning of bio-fuels

337   in high elevation area is also responsible for the presence of a large number of nitrogen-

338   containing compounds in BBOA. Nitroaromatic compounds such as Methyl-Nitrocatechols

339   ($C_7H_7NO_4$) are introduced to be tracer for biomass burning secondary organic aerosols (Iinuma

340   et al., 2010). Although $C_7H_7NO_4$ formula is not found in our measurement, $C_{14}H_{14}N_2O_8$ were

341   found in our measurement, of which is probably its dimer formula. In addition, the homologous

342   series compounds which $C_7H_7NO_4$ serve as the core molecule was also found in our samples.

343   Some medium relative abundance molecular formulas identified in a recent paper in biomass

344   burning aerosol were also found in our measurement such as $C_{15}H_{19}N_1O_8H^+$ (RI = 6.7%),

345    $C_{16}H_{21}N_1O_8H^+$ (RI = 6.6%), $C_{17}H_{23}N_1O_8H^+$ (RI = 5.9%), $C_{14}H_{13}N_1O_3H^+$ (RI = 2.9%),

346    $C_{15}H_{15}N_1O_3H^+$ (RI = 2.6%), $C_{13}H_{17}N_1O_3H^+$ (RI = 4.2%) (Song et al., 2018).

347

348   Besides primary emission and/or secondary formation from biomass burning emission, nitrogen-

349   containing OA could also be formed through other chemical processes. For example, biogenic

350   volatile organic compounds (BVOC) can react with NO_3 radical or RO_2+NO into organic nitrate

351   (Ng et al., 2017). Although organic nitrate is not favored to be ionized in positive ESI-MS (Wan

352   and Yu, 2006), organic nitrate formed from BVOC could be highly functionalized (Lee et al.,

353   2016) and ionized in positive MS through other alkaline functional groups. Recent studies have

354   shown that BVOC, including isoprene (C_5H_8) and monoterpenes ($C_{10}H_{16}$), dominate the organic

355   nitrate formation in the southeastern United States under the condition of the mixed

356   anthropogenic NO_x and BVOC (Xu et al., 2014; Lee et al., 2016; Zhang et al., 2018a). Several

357   molecular formulas formed from monoterpene and NO_3 radical were found in our study

358   ($C_9H_{13}NO_6$, $C_9H_{15}NO_6$, $C_{10}H_{17}NO_4$, $C_{10}H_{15}NO_5$, $C_{10}H_{17}NO_5$, $C_{10}H_{19}NO_5$, $C_{10}H_{15}NO_6$,

359    $C_{10}H_{17}NO_6$, $C_{10}H_{19}NO_6$,) (Lee et al., 2016; Zhang et al., 2018a). Additionally, some alkaloids,

360   such as imidazole, imidazole-2-carboxaldehyde and 1N-glyoxal-substittuted imidazole, are also

361   reported to be major products of BVOC reaction with ammonium ions or primary amines on

Atmospheric
Chemistry
and Physics
Discussions

Open Access

EGU

362 SOA (De Haan et al., 2009; Galloway et al., 2009; Updyke et al., 2012). Imidazole signal was

363 found in our HR-ToF-AMS measurement.

364

365 **4. Implications**

366 This study analyzed the WSOM using ESI(+)-FTICR-MS in fine particular aerosol from

367 Himalayas and found that the molecular compositions of WSOM were mainly comprised by

368 CHO and CHON compounds with equal important contribution. The two compounds could be

369 originated from biomass burning emission and BVOC oxidation of which many markers were

370 found in these molecular compounds. All our compounds had relatively high DBE values

371 suggesting potential high light absorption feature. Due to their relative high mass concentration

372 and high contribution of nitrogen-containing compounds (7.6% of PM_1) based on HR-ToF-AMS

373 results, it is believe that the aerosol transported to Himalayas have important application in

374 atmospheric radiative forcing and biogeochemical effects.

375

376 Ramanathan and Carmichael (2008) found distinct warming effect of light absorbing aerosol

377 over Himalayas through estimating aerosol radiative forcing by BC. However, light-absorbing

378 OA (brown carbon) could also be another important light absorbing aerosol due to their large

379 fraction of atmospheric aerosol loading (Laskin et al., 2015). Zhang et al. (2017) estimated the

380 light absorption contribution of brown carbon from inland of the TP which was up to ~13% of

381 that of BC. The high DBE and nitrogen-containing OA in our study suggested aerosol in

382 Himalayas could contain amount of light-absorbing organic matter because light absorption

383 properties of organic molecules are closely related with the number of double bonds and rings in

384 the molecule and nitrogen atoms. Many studies had found that the dominated chemical

385 molecules in the brown carbon were related with nitrogen-containing aerosol (e.g., Lin et al.,

386 2016). This kind of aerosol combined with BC could have higher radiative forcing than before in

387 this area.

388

389 In addition, nitrogen is an important nutrient for plant and microbial in terrestrial and aquatic

390 systems especially for arid and semi-arid areas (Andreae and Crutzen, 1997). Chen et al. (2013)

391 evaluated the potential biogeochemical cycle in the TP under the current rapidly climate change

392 and suggested that nitrogen availability plays a critical role in controlling ecological production

393 because nitrogen is a limited nutrient in many ecosystems. To our knowledge, there was no study

394 focusing on the organic nitrogen deposition in this remote region, but only on inorganic nitrogen

395 species (Liu et al., 2015). Organic nitrogen is an important source of nitrogen (Neff et al., 2002),

396 and should be taken account in the future study.

397

398 **Acknowledgements**

403 **References**

404 Altieri, K. E., Turpin, B. J., and Seitzinger, S. P.: Oligomers, organosulfates, and nitrooxy
405   organosulfates in rainwater identified by ultra-high resolution electrospray ionization FT-
406   ICR mass spectrometry, Atmos. Chem. Phys., 9, 2533-2542, 10.5194/acp-9-2533-2009,
407   2009a.
408 Altieri, K. E., Turpin, B. J., and Seitzinger, S. P.: Composition of Dissolved Organic Nitrogen in
409   Continental Precipitation Investigated by Ultra-High Resolution FT-ICR Mass
410   Spectrometry, Environ. Sci. Technol., 43, 6950-6955, 10.1021/es9007849, 2009b.
411 Andreae, M. O., and Crutzen, P. J.: Atmospheric Aerosols: Biogeochemical Sources and Role in
412   Atmospheric Chemistry, Science, 276, 1052-1058, 10.1126/science.276.5315.1052, 1997.
413 Bonasoni, P., Laj, P., Marinoni, A., Sprenger, M., Angelini, F., Arduini, J., Bonafè, U., Calzolari,
414   F., Colombo, T., Decesari, S., Di Biagio, C., di Sarra, A. G., Evangelisti, F., Duchi, R.,
415   Facchini, M. C., Fuzzi, S., Gobbi, G. P., Maione, M., Panday, A., Roccato, F., Sellegri,
416   K., Venzac, H., Verza, G. P., Villani, P., Vuillermoz, E., and Cristofanelli, P.:
417   Atmospheric Brown Clouds in the Himalayas: first two years of continuous observations
418   at the Nepal Climate Observatory-Pyramid (5079 m), Atmos. Chem. Phys., 10, 7515-
419   7531, 10.5194/acp-10-7515-2010, 2010.
420 Canagaratna, M. R., Jimenez, J. L., Kroll, J. H., Chen, Q., Kessler, S. H., Massoli, P.,
421   Hildebrandt Ruiz, L., Fortner, E., Williams, L. R., Wilson, K. R., Surratt, J. D., Donahue,
422   N. M., Jayne, J. T., and Worsnop, D. R.: Elemental ratio measurements of organic
423   compounds using aerosol mass spectrometry: characterization, improved calibration, and
424   implications, Atmos. Chem. Phys., 15, 253-272, 10.5194/acp-15-253-2015, 2015.
425 Chen, H., Zhu, Q., Peng, C., Wu, N., Wang, Y., Fang, X., Gao, Y., Zhu, D., Yang, G., Tian, J.,
426   Kang, X., Piao, S., Ouyang, H., Xiang, W., Luo, Z., Jiang, H., Song, X., Zhang, Y., Yu,
427   G., Zhao, X., Gong, P., Yao, T., and Wu, J.: The impacts of climate change and human
428   activities on biogeochemical cycles on the Qinghai-Tibetan Plateau, Global Change Biol.,
429   19, 2940-2955, 10.1111/gcb.12277, 2013.

430   Choi, J. H., Ryu, J., Jeon, S., Seo, J., Yang, Y. H., Pack, S. P., Choung, S., and Jang, K. S.: In-
431   depth compositional analysis of water-soluble and -insoluble organic substances in fine
432   (PM2.5) airborne particles using ultra-high-resolution 15T FT-ICR MS and GCxGC-
433   TOFMS, Environmental Pollution, 225, 329-337, 10.1016/j.envpol.2017.02.058, 2017.
434   Claeys, M., Szmigielski, R., Kourtchev, I., Van der Veken, P., Vermeylen, R., Maenhaut, W.,
435   Jaoui, M., Kleindienst, T. E., Lewandowski, M., Offenberg, J. H., and Edney, E. O.:
436   Hydroxydicarboxylic Acids: Markers for Secondary Organic Aerosol from the
437   Photooxidation of α-Pinene, Environ. Sci. Technol., 41, 1628-1634, 10.1021/es0620181,
438   2007.
439   Cong, Z., Kawamura, K., Kang, S., and Fu, P.: Penetration of biomass-burning emissions from
440   South Asia through the Himalayas: new insights from atmospheric organic acids, Sci.
441   Rep., 5, 9580, 10.1038/srep09580, 2015.
442   Cook, R. D., Lin, Y. H., Peng, Z., Boone, E., Chu, R. K., Dukett, J. E., Gunsch, M. J., Zhang,
443   W., Tolic, N., Laskin, A., and Pratt, K. A.: Biogenic, urban, and wildfire influences on
444   the molecular composition of dissolved organic compounds in cloud water, Atmos.
445   Chem. Phys., 17, 15167-15180, 10.5194/acp-17-15167-2017, 2017.
446   Cristofanelli, P., Bracci, A., Sprenger, M., Marinoni, A., Bonafè, U., Calzolari, F., Duchi, R.,
447   Laj, P., Pichon, J. M., Roccato, F., Venzac, H., Vuillermoz, E., and Bonasoni, P.:
448   Tropospheric ozone variations at the Nepal Climate Observatory-Pyramid (Himalayas,
449   5079 m a.s.l.) and influence of deep stratospheric intrusion events, Atmos. Chem. Phys.,
450   10, 6537-6549, 10.5194/acp-10-6537-2010, 2010.
451   De Haan, D. O., Corrigan, A. L., Tolbert, M. A., Jimenez, J. L., Wood, S. E., and Turley, J. J.:
452   Secondary Organic Aerosol Formation by Self-Reactions of Methylglyoxal and Glyoxal
453   in Evaporating Droplets, Environ. Sci. Technol., 43, 8184-8190, 10.1021/es902152t,
454   2009.
455   Draxler, R. R., and Hess, G. D.: An overview of the hysplit-4 modeling system for trajectories,
456   Aust. Meteorol. Mag., 47, 295-308, 1998.
457   Dzepina, K., Mazzoleni, C., Fialho, P., China, S., Zhang, B., Owen, R. C., Helmig, D., Hueber,
458   J., Kumar, S., Perlinger, J. A., Kramer, L. J., Dziobak, M. P., Ampadu, M. T., Olsen, S.,
459   Wuebbles, D. J., and Mazzoleni, L. R.: Molecular characterization of free tropospheric
460   aerosol collected at the Pico Mountain Observatory: a case study with a long-range
461   transported biomass burning plume, Atmos. Chem. Phys., 15, 5047-5068, 10.5194/acp-
462   15-5047-2015, 2015.
463   Feng, L., Xu, J., Kang, S., Li, X., Li, Y., Jiang, B., and Shi, Q.: Chemical Composition of
464   Microbe-Derived Dissolved Organic Matter in Cryoconite in Tibetan Plateau Glaciers:
465   Insights from Fourier Transform Ion Cyclotron Resonance Mass Spectrometry Analysis,
466   Environ Sci Technol, 50, 13215-13223, 10.1021/acs.est.6b03971, 2016.
467   Fleming, L. T., Lin, P., Laskin, A., Laskin, J., Weltman, R., Edwards, R. D., Arora, N. K.,
468   Yadav, A., Meinardi, S., Blake, D. R., Pillarisetti, A., Smith, K. R., and Nizkorodov, S.
469   A.: Molecular composition of particulate matter emissions from dung and brushwood
470   burning household cookstoves in Haryana, India, Atmos. Chem. Phys., 18, 2461-2480,
471   10.5194/acp-18-2461-2018, 2018.
472   Galloway, M. M., Chhabra, P. S., Chan, A. W. H., Surratt, J. D., Flagan, R. C., Seinfeld, J. H.,
473   and Keutsch, F. N.: Glyoxal uptake on ammonium sulphate seed aerosol: reaction

Atmospheric
Chemistry
and Physics
Discussions

474   products and reversibility of uptake under dark and irradiated conditions, Atmos. Chem.
475   Phys., 9, 3331-3345, 10.5194/acp-9-3331-2009, 2009.
476 Gustafsson, Ö., Kruså, M., Zencak, Z., Sheesley, R. J., Granat, L., Engström, E., Praveen, P. S.,
477   Rao, P. S. P., Leck, C., and Rodhe, H.: Brown Clouds over South Asia: Biomass or Fossil
478   Fuel Combustion?, Science, 323, 495-498, 10.1126/science.1164857, 2009.
479 Hoffmann, D., Iinuma, Y., and Herrmann, H.: Development of a method for fast analysis of
480   phenolic molecular markers in biomass burning particles using high performance liquid
481   chromatography/atmospheric pressure chemical ionisation mass spectrometry, J.
482   Chromatogr. A, 1143, 168-175, 10.1016/j.chroma.2007.01.035, 2007.
483 Hughey, C. A., Hendrickson, C. L., Rodgers, R. P., Marshall, A. G., and Qian, K.: Kendrick
484   Mass Defect Spectrum: A Compact Visual Analysis for Ultrahigh-Resolution Broadband
485   Mass Spectra, Anal. Chem., 73, 4676-4681, 10.1021/ac010560w, 2001.
486 Iinuma, Y., Böge, O., Gräfe, R., and Herrmann, H.: Methyl-Nitrocatechols: Atmospheric Tracer
487   Compounds for Biomass Burning Secondary Organic Aerosols, Environ. Sci. Technol.,
488   44, 8453-8459, 10.1021/es102938a, 2010.
489 Jayarathne, T., Stockwell, C. E., Bhave, P. V., Praveen, P. S., Rathnayake, C. M., Islam, M. R.,
490   Panday, A. K., Adhikari, S., Maharjan, R., Goetz, J. D., DeCarlo, P. F., Saikawa, E.,
491   Yokelson, R. J., and Stone, E. A.: Nepal Ambient Monitoring and Source Testing
492   Experiment (NAMaSTE): emissions of particulate matter from wood- and dung-fueled
493   cooking fires, garbage and crop residue burning, brick kilns, and other sources, Atmos.
494   Chem. Phys., 18, 2259-2286, 10.5194/acp-18-2259-2018, 2018.
495 Kleindienst, T. E., Jaoui, M., Lewandowski, M., Offenberg, J. H., Lewis, C. W., Bhave, P. V.,
496   and Edney, E. O.: Estimates of the contributions of biogenic and anthropogenic
497   hydrocarbons to secondary organic aerosol at a southeastern US location, Atmos.
498   Environ., 41, 8288-8300, 10.1016/j.atmosenv.2007.06.045, 2007.
499 Koch, B. P., and Dittmar, T.: From mass to structure: an aromaticity index for high-resolution
500   mass data of natural organic matter, Rapid Commun. Mass. Sp, 20, 926-932,
501   10.1002/rcm.2386, 2006.
502 Kristensen, K., Enggrob, K. L., King, S. M., Worton, D. R., Platt, S. M., Mortensen, R.,
503   Rosenoern, T., Surratt, J. D., Bilde, M., Goldstein, A. H., and Glasius, M.: Formation and
504   occurrence of dimer esters of pinene oxidation products in atmospheric aerosols, Atmos.
505   Chem. Phys., 13, 3763-3776, 10.5194/acp-13-3763-2013, 2013.
506 Laskin, A., Smith, J. S., and Laskin, J.: Molecular Characterization of Nitrogen-Containing
507   Organic Compounds in Biomass Burning Aerosols Using High-Resolution Mass
508   Spectrometry, Environ. Sci. Technol., 43, 3764-3771, 10.1021/es803456n, 2009.
509 Laskin, A., Laskin, J., and Nizkorodov, S. A.: Chemistry of Atmospheric Brown Carbon, Chem.
510   Rev., 4335-4382, 10.1021/cr5006167, 2015.
511 Laskin, J., Laskin, A., and Nizkorodov, S. A.: Mass Spectrometry Analysis in Atmospheric
512   Chemistry, Anal. Chem., 90, 166-189, 10.1021/acs.analchem.7b04249, 2018.
513 Lau, K. M., Kim, M. K., and Kim, K. M.: Asian summer monsoon anomalies induced by aerosol
514   direct forcing: the role of the Tibetan Plateau, Clim. Dynam., 26, 855-864,
515   10.1007/s00382-006-0114-z, 2006.
516 Lee, B. H., Mohr, C., Lopez-Hilfiker, F. D., Lutz, A., Hallquist, M., Lee, L., Romer, P., Cohen,
517   R. C., Iyer, S., Kurtén, T., Hu, W., Day, D. A., Campuzano-Jost, P., Jimenez, J. L., Xu,
518   L., Ng, N. L., Guo, H., Weber, R. J., Wild, R. J., Brown, S. S., Koss, A., de Gouw, J.,

519   Olson, K., Goldstein, A. H., Seco, R., Kim, S., McAvey, K., Shepson, P. B., Starn, T.,
520   Baumann, K., Edgerton, E. S., Liu, J., Shilling, J. E., Miller, D. O., Brune, W.,
521   Schobesberger, S., D'Ambro, E. L., and Thornton, J. A.: Highly functionalized organic
522   nitrates in the southeast United States: Contribution to secondary organic aerosol and
523   reactive nitrogen budgets, Proc. Natl. Acad. Sci. USA.,, 113, 1516-1521,
524   10.1073/pnas.1508108113, 2016.
525 Lin, P., Rincon, A. G., Kalberer, M., and Yu, J. Z.: Elemental Composition of HULIS in the
526   Pearl River Delta Region, China: Results Inferred from Positive and Negative
527   Electrospray High Resolution Mass Spectrometric Data, Environ. Sci. Technol., 46,
528   7454-7462, 10.1021/es300285d, 2012.
529 Lin, P., Aiona, P. K., Li, Y., Shiraiwa, M., Laskin, J., Nizkorodov, S. A., and Laskin, A.:
530   Molecular Characterization of Brown Carbon in Biomass Burning Aerosol Particles,
531   Environ. Sci. Technol., 50, 11815-11824, 10.1021/acs.est.6b03024, 2016.
532 Liu, Y. W., Xu, R., Wang, Y. S., Pan, Y. P., and Piao, S. L.: Wet deposition of atmospheric
533   inorganic nitrogen at five remote sites in the Tibetan Plateau, Atmos. Chem. Phys., 15,
534   11683-11700, 10.5194/acp-15-11683-2015, 2015.
535 Liu, Z., Liu, D., Huang, J., Vaughan, M., Uno, I., Sugimoto, N., Kittaka, C., Trepte, C., Wang,
536   Z., Hostetler, C., and Winker, D.: Airborne dust distributions over the Tibetan Plateau
537   and surrounding areas derived from the first year of CALIPSO lidar observations, Atmos.
538   Chem. Phys., 8, 5045-5060, 10.5194/acp-8-5045-2008, 2008.
539 Lu, Z., Streets, D. G., Zhang, Q., and Wang, S.: A novel back-trajectory analysis of the origin of
540   black carbon transported to the Himalayas and Tibetan Plateau during 1996–2010,
541   Geophys. Res. Lett., 39, L01809, 10.1029/2011gl049903, 2012.
542 Lüthi, Z. L., Škerlak, B., Kim, S. W., Lauer, A., Mues, A., Rupakheti, M., and Kang, S.:
543   Atmospheric brown clouds reach the Tibetan Plateau by crossing the Himalayas, Atmos.
544   Chem. Phys., 15, 6007-6021, 10.5194/acp-15-6007-2015, 2015.
545 Mazzoleni, L. R., Ehrmann, B. M., Shen, X., Marshall, A. G., and Collett, J. L.: Water-Soluble
546   Atmospheric Organic Matter in Fog: Exact Masses and Chemical Formula Identification
547   by Ultrahigh-Resolution Fourier Transform Ion Cyclotron Resonance Mass
548   Spectrometry, Environ. Sci. Technol., 44, 3690-3697, 10.1021/es903409k, 2010.
549 Mazzoleni, L. R., Saranjampour, P., Dalbec, M. M., Samburova, V., Hallar, A. G., Zielinska, B.,
550   Lowenthal, D. H., and Kohl, S.: Identification of water-soluble organic carbon in non-
551   urban aerosols using ultrahigh-resolution FT-ICR mass spectrometry: organic anions,
552   Environ. Chem., 9, 285, 10.1071/en11167, 2012.
553 Neff, J. C., Holland, E. A., Dentener, F. J., McDowell, W. H., and Russell, K. M.: The origin,
554   composition and rates of organic nitrogen deposition: A missing piece of the nitrogen
555   cycle?, Biogeochemistry, 57, 99-136, 10.1023/a:1015791622742, 2002.
556 Ng, N. L., Brown, S. S., Archibald, A. T., Atlas, E., Cohen, R. C., Crowley, J. N., Day, D. A.,
557   Donahue, N. M., Fry, J. L., Fuchs, H., Griffin, R. J., Guzman, M. I., Herrmann, H.,
558   Hodzic, A., Iinuma, Y., Jimenez, J. L., Kiendler-Scharr, A., Lee, B. H., Luecken, D. J.,
559   Mao, J., McLaren, R., Mutzel, A., Osthoff, H. D., Ouyang, B., Picquet-Varrault, B., Platt,
560   U., Pye, H. O. T., Rudich, Y., Schwantes, R. H., Shiraiwa, M., Stutz, J., Thornton, J. A.,
561   Tilgner, A., Williams, B. J., and Zaveri, R. A.: Nitrate radicals and biogenic volatile
562   organic compounds: oxidation, mechanisms, and organic aerosol, Atmos. Chem. Phys.,
563   17, 2103-2162, 10.5194/acp-17-2103-2017, 2017.

564 O'Brien, R. E., Laskin, A., Laskin, J., Liu, S., Weber, R., Russell, L. M., and Goldstein, A. H.:
565   Molecular characterization of organic aerosol using nanospray desorption/electrospray
566   ionization mass spectrometry: CalNex 2010 field study, Atmos. Environ., 68, 265-272,
567   10.1016/j.atmosenv.2012.11.056, 2013.
568 Ram, K., Sarin, M. M., and Hegde, P.: Long-term record of aerosol optical properties and
569   chemical composition from a high-altitude site (Manora Peak) in Central Himalaya,
570   Atmos. Chem. Phys., 10, 11791-11803, 10.5194/acp-10-11791-2010, 2010.
571 Ramanathan, V., Ramana, M. V., Roberts, G., Kim, D., Corrigan, C., Chung, C., and Winker, D.:
572   Warming trends in Asia amplified by brown cloud solar absorption, Nature, 448, 575-
573   578, 10.1038/nature06019, 2007.
574 Ramanathan, V., and Carmichael, G.: Global and regional climate changes due to black carbon,
575   Nature Geos., 1, 221-227, 10.1038/ngeo156, 2008.
576 Saleh, R., Robinson, E. S., Tkacik, D. S., Ahern, A. T., Liu, S., Aiken, A. C., Sullivan, R. C.,
577   Presto, A. A., Dubey, M. K., Yokelson, R. J., Donahue, N. M., and Robinson, A. L.:
578   Brownness of organics in aerosols from biomass burning linked to their black carbon
579   content, Nature Geos., 7, 647-650, 10.1038/ngeo2220, 2014.
580 Schmitt-Kopplin, P., Liger-Belair, G., Koch, B. P., Flerus, R., Kattner, G., Harir, M., Kanawati,
581   B., Lucio, M., Tziotis, D., Hertkorn, N., and Gebefügi, I.: Dissolved organic matter in sea
582   spray: a transfer study from marine surface water to aerosols, Biogeosciences, 9, 1571-
583   1582, 10.5194/bg-9-1571-2012, 2012.
584 Smith, J. S., Laskin, A., and Laskin, J.: Molecular Characterization of Biomass Burning Aerosols
585   Using High-Resolution Mass Spectrometry, Anal. Chem., 81, 1512-1521,
586   10.1021/ac8020664, 2009.
587 Song, J., Li, M., Jiang, B., Wei, S., Fan, X., and Peng, P. a.: Molecular Characterization of
588   Water-Soluble Humic like Substances in Smoke Particles Emitted from Combustion of
589   Biomass Materials and Coal Using Ultrahigh-Resolution Electrospray Ionization Fourier
590   Transform Ion Cyclotron Resonance Mass Spectrometry, Environ. Sci. Technol., 52,
591   2575-2585, 10.1021/acs.est.7b06126, 2018.
592 Stockwell, C. E., Christian, T. J., Goetz, J. D., Jayarathne, T., Bhave, P. V., Praveen, P. S.,
593   Adhikari, S., Maharjan, R., DeCarlo, P. F., Stone, E. A., Saikawa, E., Blake, D. R.,
594   Simpson, I. J., Yokelson, R. J., and Panday, A. K.: Nepal Ambient Monitoring and
595   Source Testing Experiment (NAMaSTE): emissions of trace gases and light-absorbing
596   carbon from wood and dung cooking fires, garbage and crop residue burning, brick kilns,
597   and other sources, Atmos. Chem. Phys., 16, 11043-11081, 10.5194/acp-16-11043-2016,
598   2016.
599 Stone, E. A., Nguyen, T. T., Pradhan, B. B., and Man Dangol, P.: Assessment of biogenic
600   secondary organic aerosol in the Himalayas, Environ. Chem., 9, 263-272,
601   10.1071/EN12002, 2012.
602 Sun, Y. L., Zhang, Q., Anastasio, C., and Sun, J.: Insights into secondary organic aerosol formed
603   via aqueous-phase reactions of phenolic compounds based on high resolution mass
604   spectrometry, Atmos. Chem. Phys., 10, 4809-4822, 10.5194/acp-10-4809-2010, 2010.
605 Updyke, K. M., Nguyen, T. B., and Nizkorodov, S. A.: Formation of brown carbon via reactions
606   of ammonia with secondary organic aerosols from biogenic and anthropogenic
607   precursors, Atmos. Environ., 63, 22-31, 10.1016/j.atmosenv.2012.09.012, 2012.

608   Wan, E. C. H., and Yu, J. Z.: Determination of sugar compounds in atmospheric aerosols by
609   liquid chromatography combined with positive electrospray ionization mass
610   spectrometry, J. Chromatogr. A, 1107, 175-181, 10.1016/j.chroma.2005.12.062, 2006.
611   Wang, X., Gong, P., Sheng, J., Joswiak, D. R., and Yao, T.: Long-range atmospheric transport of
612   particulate Polycyclic Aromatic Hydrocarbons and the incursion of aerosols to the
613   southeast Tibetan Plateau, Atmos. Environ., 115, 124-131,
614   10.1016/j.atmosenv.2015.04.050, 2015.
615   Wang, X., Ren, J., Gong, P., Wang, C., Xue, Y., Yao, T., and Lohmann, R.: Spatial distribution
616   of the persistent organic pollutants across the Tibetan Plateau and its linkage with the
617   climate systems: a 5-year air monitoring study, Atmos. Chem. Phys., 16, 6901-6911,
618   10.5194/acp-16-6901-2016, 2016.
619   Wozniak, A. S., Bauer, J. E., Sleighter, R. L., Dickhut, R. M., and Hatcher, P. G.: Technical
620   Note: Molecular characterization of aerosol-derived water soluble organic carbon using
621   ultrahigh resolution electrospray ionization Fourier transform ion cyclotron resonance
622   mass spectrometry, Atmos. Chem. Phys., 8, 5099-5111, 10.5194/acp-8-5099-2008, 2008.
623   Wozniak, A. S., Willoughby, A. S., Gurganus, S. C., and Hatcher, P. G.: Distinguishing
624   molecular characteristics of aerosol water soluble organic matter from the 2011 trans-
625   North Atlantic US GEOTRACES cruise, Atmos. Chem. Phys., 14, 8419-8434,
626   10.5194/acp-14-8419-2014, 2014.
627   Wu, Z., Rodgers, R. P., and Marshall, A. G.: Two- and three-dimensional van krevelen diagrams:
628   a graphical analysis complementary to the kendrick mass plot for sorting elemental
629   compositions of complex organic mixtures based on ultrahigh-resolution broadband
630   fourier transform ion cyclotron resonance, Anal. Chem., 76, 2511-2516,
631   10.1021/ac0355449, 2004.
632   Xia, X., Zong, X., Cong, Z., Chen, H., Kang, S., and Wang, P.: Baseline continental aerosol over
633   the central Tibetan plateau and a case study of aerosol transport from South Asia, Atmos.
634   Environ., 45, 7370-7378, 10.1016/j.atmosenv.2011.07.067, 2011.
635   Xu, J., Zhang, Q., Shi, J., Ge, X., Xie, C., Wang, J., Kang, S., Zhang, R., and Wang, Y.:
636   Chemical characteristics of submicron particles at the central Tibetan Plateau: insights
637   from aerosol mass spectrometry, Atmos. Chem. Phys., 18, 427-443, 10.5194/acp-18-427-
638   2018, 2018.
639   Xu, L., Guo, H., Boyd, C. M., Klein, M., Bougiatioti, A., Cerully, K. M., Hite, J. R., Isaacman-
640   VanWertz, G., Kreisberg, N. M., Knote, C., Olson, K., Koss, A., Goldstein, A. H.,
641   Hering, S. V., de Gouw, J., Baumann, K., Lee, S.-H., Nenes, A., Weber, R. J., and Ng, N.
642   L.: Effects of anthropogenic emissions on aerosol formation from isoprene and
643   monoterpenes in the southeastern United States, Proc. Natl. Acad. Sci. USA.,
644   10.1073/pnas.1417609112, 2014.
645   Yu, L., Smith, J., Laskin, A., Anastasio, C., Laskin, J., and Zhang, Q.: Chemical characterization
646   of SOA formed from aqueous-phase reactions of phenols with the triplet excited state of
647   carbonyl and hydroxyl radical, Atmos. Chem. Phys., 14, 13801-13816, 10.5194/acp-14-
648   13801-2014, 2014.
649   Yu, L., Smith, J., Laskin, A., George, K. M., Anastasio, C., Laskin, J., Dillner, A. M., and
650   Zhang, Q.: Molecular transformations of phenolic SOA during photochemical aging in
651   the aqueous phase: competition among oligomerization, functionalization, and
652   fragmentation, Atmos. Chem. Phys., 16, 4511-4527, 10.5194/acp-16-4511-2016, 2016.

653 Zhang, H., Yee, L. D., Lee, B. H., Curtis, M. P., Worton, D. R., Isaacman-VanWertz, G.,
654   Offenberg, J. H., Lewandowski, M., Kleindienst, T. E., Beaver, M. R., Holder, A. L.,
655   Lonneman, W. A., Docherty, K. S., Jaoui, M., Pye, H. O. T., Hu, W., Day, D. A.,
656   Campuzano-Jost, P., Jimenez, J. L., Guo, H., Weber, R. J., de Gouw, J., Koss, A. R.,
657   Edgerton, E. S., Brune, W., Mohr, C., Lopez-Hilfiker, F. D., Lutz, A., Kreisberg, N. M.,
658   Spielman, S. R., Hering, S. V., Wilson, K. R., Thornton, J. A., and Goldstein, A. H.:
659   Monoterpenes are the largest source of summertime organic aerosol in the southeastern
660   United States, Proc. Natl. Acad. Sci. USA.,, 115, 2038-2043, 10.1073/pnas.1717513115,
661   2018a.
662 Zhang, R., Wang, H., Qian, Y., Rasch, P. J., Easter, R. C., Ma, P. L., Singh, B., Huang, J., and
663   Fu, Q.: Quantifying sources, transport, deposition, and radiative forcing of black carbon
664   over the Himalayas and Tibetan Plateau, Atmos. Chem. Phys., 15, 6205-6223,
665   10.5194/acp-15-6205-2015, 2015.
666 Zhang, X., Xu, J., Kang, S., Liu, Y., and Zhang, Q.: Chemical characterization of long-range
667   transport biomass burning emissions to the Himalayas: insights from high-resolution
668   aerosol mass spectrometry, Atmos. Chem. Phys., 18, 4617-4638, 10.5194/acp-18-4617-
669   2018, 2018b.
670 Zhang, Y., Xu, J., Shi, J., Xie, C., Ge, X., Wang, J., Kang, S., and Zhang, Q.: Light absorption by
671   water-soluble organic carbon in atmospheric fine particles in the central Tibetan Plateau,
672   Environ. Sci. Pollut. Res., 24, 21386-21397, 10.1007/s11356-017-9688-8, 2017.
673 Zhao, Y., Hallar, A. G., and Mazzoleni, L. R.: Atmospheric organic matter in clouds: exact
674   masses and molecular formula identification using ultrahigh-resolution FT-ICR mass
675   spectrometry, Atmos. Chem. Phys., 13, 12343-12362, 10.5194/acp-13-12343-2013, 2013.
676

677

678   Tables 1. Chemical characterization of the molecular assignments detected in WSOM for F30,

679   F43, and common ions. Relative intensity weighted (w) each data subset (O/C, H/C, OM/OC,

680   DBE, and DBE/C) are given.

		All	CHO	CHON
F30	O / C_w	0.43	0.43	0.42
	H / C_w	1.38	1.40	1.35
	OM / OC_w	1.72	1.69	1.77
	DBE_w	6.26	6.00	6.69
	DBE / C_w	0.34	0.32	0.36
	Number of Aliphatic (AI = 0)	2602	1514	1088
	Olefinic (0.5 > AI >0)	1584	708	876
	Aromatic (AI >= 0.5)	123	75	48
F43	O / C_w	0.38	0.38	0.39
	H / C_w	1.33	1.35	1.31
	OM / OC_w	1.67	1.62	1.72
	DBE_w	6.92	6.36	7.46
	DBE / C_w	0.36	0.34	0.38
	Number of Aliphatic (AI = 0)	2413	1200	1213
	Olefinic (0.5 > AI >0)	2256	870	1306
	Aromatic (AI >= 0.5)	249	103	146
Common ions	O / C_w	0.41	0.43	0.40
	H / C_w	1.36	1.34	1.37
	OM / OC_w	1.70	1.65	1.76
	DBE_w	6.33	5.96	6.79
	DBE / C_w	0.34	0.33	0.37
	Number of Aliphatic (AI = 0)	2067	1019	1048
	Olefinic (0.5 > AI >0)	1518	653	865
	Aromatic (AI >= 0.5)	112	71	41

681

682

683

684   Table 2. Chemical characterization of the molecular assignments detected in aerosol samples

685   from selected studies (adapted and modified from Table 3 in Dzepina et al. (2015)). Note that all
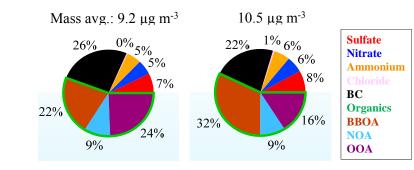
686   values are presented as arithmetic mean.

Sample type	Measurement site	Instrument	O / C	H / C	OM / OC	DBE	DBE / C	Reference
Aerosol	Free troposphere	ESI(+)-FTICR-MS	0.38–0.42	1.27–1.31	1.66–1.71	7.73–8.62	0.36–0.37	This study
Aerosol	Free troposphere	ESI(−)-FTICR-MS	0.42–0.46	1.17–1.28	1.67–1.73	9.4–10.7	0.42–0.47	Dzepina et al. (2015)
Aerosol	Free troposphere	ESI(−)-FTICR-MS	0.53 ± 0.2	1.48 ± 0.3	1.91 ± 0.3	6.18 ± 3.0	/	Mazzoleni et al. (2012)
Aerosol	Rural	ESI(−)-FTICR-MS	0.28–0.32	1.37–1.46	1.54–1.60	6.30–7.45	0.33–0.38	Wozniak et al. (2008)
Aerosol	Suburban	ESI(−)-FTICR-MS	0.46	1.34	1.85	5.3	0.45	Lin et al. (2012)
Aerosol	Urban	ESI(+)-FTICR-MS	0.31	1.34	/	8.68	0.41	Choi et al. (2017)
Aerosol	Marin boundary layer	ESI(−)-FTICR-MS	0.35	1.59	1.67	4.37	0.28	Schmitt-Kopplin et al. (2012)
Aerosol	Marine boundary layer	ESI(−)-FTICR-MS	0.36 –0.42	1.49–1.56	1.70–1.74	5.88–6.76	0.28–0.32	Wozniak et al. (2014)
Cloud water	Free troposphere	ESI(−)-FTICR-MS	0.61–0.62	1.46	2.06–2.08	6.29–6.30	0.38	Zhao et al. (2013)
Cloud water	Rural	ESI(−)-FTICR-MS	0.51	1.47	/	6.03	/	Cook et al. (2017)
Fog water	Rural	ESI(−)-FTICR-MS	0.43	1.39	1.77	5.6	0.40	Mazzoleni et al. (2010)

687

688

689

690

691 Fig. 1. The average mass concentration and chemical composition of PM$_1$ during F30 (left) and

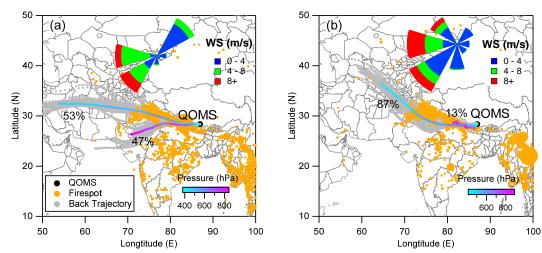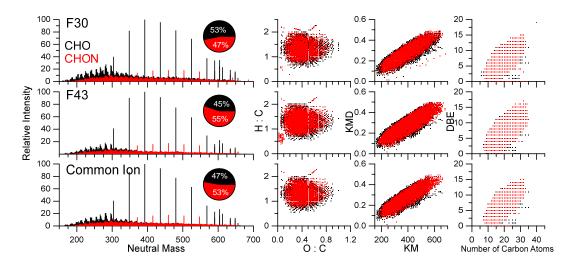692 F43 (right) periods, respectively, measured by HR-ToF-AMS and PAX.

693

694

695

Fig. 2. The air mass back trajectory analysis using HYSPLIT model (Draxler and Hess, 1998) during (a) F30 and (b) F43. The air mass trajectories were recovered back to 72 h at 1 h interval from the sampling site (QOMS) above the ground level of 1000 m using 1° resolution Global Data Assimilation System (GDAS) dataset (https://ready.arl.noaa.gov/gdas1.php). The cluster analysis for these trajectories was completed based on the directions of the trajectories (angle distance) and colored according to air pressure. The fire spot observed from MODIS (https://firms.modaps.eosdis.nasa.gov) and the average wind rose plot for during each filter sampling period were also shown. The fire spot is sized by fire radiative power (FRP).

704

705

Fig. 3. The combo plot for F30, F43, and Common Ion including high-resolution mass spectrum,

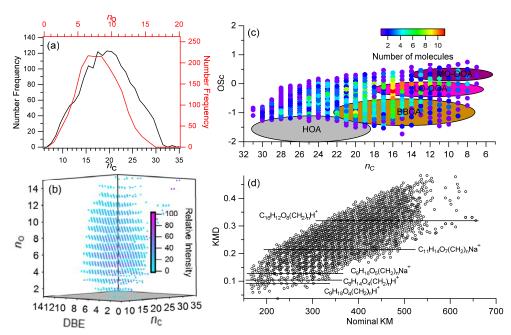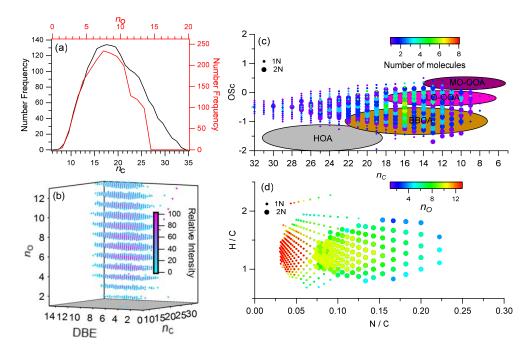707   Van Krevelen diagram, KMD vs. KM, and DBE vs. number of carbon atoms.

708

709

710

711   Fig. 4. The molecular information for common CHO compounds of two filters. (a) The number

712   frequency distribution of carbon (n_c) and oxygen (n_o); (b) The 3-D plot for n_o, n_c, and DBE

713   colored by their relative intensity; (c) Scatter plot of carbon based oxidation state (OSc) vs. nc

714   colored by the distribution of number of molecules; (d) The Van Kerevelen diagram by H/C vs.

715   N/C colored by no. The size of dot marker in (c) and (d) represent the 1N and 2N compounds.

716

717

718   Fig. 5. The molecular information for common CHON compounds of two filters. (a) The number

719   frequency distribution of carbon (n_c) and oxygen (n_o). (b) The 3-D plot for n_o, n_c, and DBE

720   colored by their relative intensity. (c) Scatter plot of carbon based oxidation state (OSc) vs. nc

721   colored by the distribution of number of molecules. (d) The Van Kerevelen diagram by H/C vs.

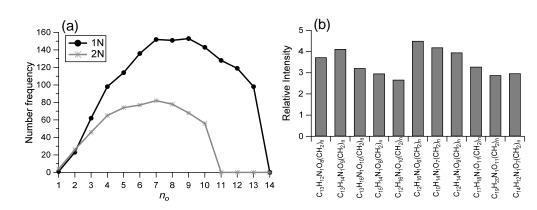722   N/C colored by no. The size of dot marker in (c) and (d) represent the 1N and 2N compounds.

723

Atmospheric
Chemistry
and Physics
Discussions

724

725

726   Fig. 6. (a) The number frequency distribution of n_o for 1N and 2N compounds and (b) the longest

727   ten CH2 homologous series compounds in 1N compounds.

728